

Investigation of Tensile Strength and Modulus of PVA/CuO/CdS Nanocomposite Films using Mathematical Models

Koteswararao Jammula^{*1}, Madhu G M¹, V Venkatesham² and Venkata Satyanarayana Suggala³

¹Department of Chemical Engineering, MS Ramaiah Institute of Technology, Bangalore 560 054, Karnataka, India.

²Department of Chemical Engineering, Adhiyamaan College of Engineering, Hosur 635109, Tamil Nadu, India

³Department of Chemical Engineering, JNTUA College of Engineering, Ananthapuramu 515 002, Andhra Pradesh, India

Abstract

Present work has been directed to test the effect of nanometal filler loading/concentration (CuO and CdS) into a PVA matrix to improve the mechanical properties of the PVA for strengthening purposes. The nanometal fillers synthesized by solution combustion and hydrothermal methods were used. The polymer nanocomposite films were cast by solution intercalation technique with varying amounts of 0.5, 1.0, 1.5, and 2.0 %wt. of nanofiller content. Theoretical models can be used to verify the relative Young's modulus and relative tensile strength. The Nicolais-Narkis and Turcsenyi models, which were put to the test, exhibit excellent agreement with the experimental values of relative tensile strength. Compared to experimental values of relatively Young's modulus, the Kerner and Halpin-Tsai models agree well. It is corroborated by the theoretical models that CuO and PVA interact well, increasing the mechanical characteristics of films when filler loading is increased. For nano CdS-PVA composite films, theoretical models, including Piggot-Leidner, Turcsenyi, Nelsen, and Nicolais-Narkis, were investigated. Nicolais-Narkis and Turcsenyi models are in excellent agreement with experimental values for relative tensile strength. The relative Young's modulus was predicted using the models developed by Kerner, Halpin-Tsai, and Sato-Furukawa. All of the studied models show strong agreement with the results of the experiments.

Keywords: Mathematical models, Relative Tensile Strength, Relative Young's Modulus, Copper Oxide, Cadmium Sulfide

1.0 Introduction

There are several different types of nanomaterials, including tubes, particles, rods, and fibres, all of which have an external length of at least 100 nm. (less/inside structures measuring 100 nm). These materials are accessible in bulk form and share the same composition as related materials that have a diversity of physicochemical characteristics. The size, shape, surface area, size distribution, crystallinity, and purity of produced nanoparticles must all be controlled in order to

create bigger nanostructures, as the properties of nanomaterials depend not only on composition but also on size and form. Metal oxides are corrosion-resistant (coated) and have been employed in the production of catalysts, sensors, fuel cells, microelectronic circuits, and piezoelectric devices^{1,2,3,4,5}. When combined with or doped with other materials, metal oxide nanoparticles exhibit distinct chemical and physical characteristics^{6,7}.

Metals can exhibit a wide spectrum of electrical characteristics when incorporated into polymers, from semiconductors to metal. Heat-sensitive, flexible, electrically insulating, and biomedical materials are all classified as

^{*}Author for correspondence

polymers. These conducting polymers offer advantages over metals and saturated carbon composites due to their insulating characteristics, as well as being lightweight, resistant to corrosion, and processable. Essential qualities, including low density, manufacturing, and material flexibility, were started to modify the polymer architectures and add new additives to chemically and mechanically manufacture various kinds of inorganic nano-filler dispersed polymers. However, these methods require modifying the nano-filler surfaces and/or the nanocomposites' polymerization processes⁸.

It is normally necessary to distinguish the mechanical characteristics of nanocomposites from various angles to improve the stability of polymer nanocomposite films with toughness and stiffness. Using a commonly used tensile test, data on tensile strength, elongation, and Young's modulus are gathered at the break to evaluate the mechanical characteristics of the resulting polymer nanocomposites. Depending on the application, the mechanical characteristics of polymer composites that contain nanoparticles may be changed or even improved. Increased Young's modulus, tensile strength, stiffness, or elasticity are some examples of these characteristics⁹.

The high-density polyethylene (HDPE)-fly ash cenospheres composites were obtained at 210°C by blending HDPE, HDPE-g-DBM compatibilizer, and cenosphere with various volume fractions of filler. The mechanical properties of HDPE-fly ash cenospheres composites were tested using a tensile tester (Model H-50k, tensile test executed as per ASTM D 1708)¹⁰. The experimental results estimated from the test such as relative tensile strength (RTS) and relative Young's modulus (RYM) values. These experimental values match with the mathematical models for enhancement to the thermal stability and mechanical properties of composites. The experimental results (RTS) have been investigated by three mathematical models, Nicolais and Narkis, Halpin-Tsai, and Turcsanyi, for theoretical prediction¹¹. Trial and error is used to obtain at model parameter values that match experimental values. These values (either increases or decreases) can be suggested that may affect the interfacial bond. Another work was carried out on the relative Young's modulus (RYM) values with theoretical models such as Kerner's, Halpin-Tsai and Sato, and Furukawa¹². From these models, the reported values are not matched with the experimental values as they assume no interface between the filler and matrix. The match between experimental values the theoretically predicted values indicates improved interfacial bond due to enhanced scattering of filler in the matrix^{13,14}.

Studies of polymer nanocomposite films made employing the casting process and raw ingredients like graphene mixed with water-soluble polymers (The authors published research on poly vinyl alcohol (PVA) and polyethylene glycol (PEG)¹⁵. Fourier transform infrared spectroscopy (FTIR), differential scanning calorimetry (DSC), methods were used to

characterize the fabricated films. Mechanical properties were studied using a universal tensile machine for calculating tensile strength. The theoretically predictive model (Nicolais and Narkis) values were matched with the experimental values of tensile strength.

The PVA-Graphene oxide nanocomposite films were prepared with starting materials of graphene oxide mixing with the PVA matrix using a water solution processing technique. The stress-strain relations analyzed between the polymer matrix and graphene oxide. The mechanical performance reported the strong improvement in an interfacial bond due to the H bond connecting the PVA matrix and graphene. The theoretically estimated Young's modulus values from Halpin-Tsai model, it's matched with the experimental values¹⁶.

The current study's goals are to synthesize copper oxide and cadmium sulfide nanoparticles using hydrothermal and solution combustion processes, respectively. Fabrication of nano CuO-PVA and CdS-PVA polymer composite films loaded with a different weight percentage of nanofillers. Use the predicted values of mechanical properties from the models to compare with experimental mechanical properties, such as the relative tensile strength and relative Young's modulus of the fabricated films.

2.0 Mathematical Modelling

Mathematical models discussed in the present work are used to compare the experimental observations of mechanical properties and stress-strain curves with theoretical methodology. The values of tensile strength and Young's modulus for interphase relations between the filler and polymer matrix were obtained. It is advised to use a multi-phase model with nanofillers, a polymer matrix, and identified interfacial sections. The main novelties listed below have been utilised in the current work, totaling seven new mathematical models that are relevant to empirical relations.

The Piggot-Leidner, Nicolais-Narkis, Turcsanyi, and Nielsen mathematical models were taken into consideration to study the mechanical property of relative tensile strength (RTS) of polymer nanocomposites. A different set of models was studied relative Young's modulus (RYM). Models are Kerner, Halpin-Tsai, and Sato-Furukawa. The physical properties of material data required for theoretical models are

Table 1: Materials used in polymer nanocomposites for mathematical models

Material	PVA	CuO	CdS
Aspect ratio (Af)	430	5.71	10
Passion ratio (v)	0.45	0.44	0.4
Density (kg/m ³)	1190	6315	4826

given in Error! Reference source not found.

Four theoretical models are employed using a trial-and-error method to determine if the relative tensile strength (RTS) matches the experimental data¹⁷. The model's parameter values obtained are discussed below.

Model 1: by Nicolais-Narkis¹⁸ is provided in Equation (2.1).

$$\text{RTS} = 1 - K(\phi')^2 \quad (2.1)$$

The volume per cent of CuO is indicated in Equation (2.1) by the symbol (ϕ') , which is provided below the Equation.

$$\phi_i = \frac{\left(\frac{w_i}{\rho_i}\right)}{\sum \left(\frac{w_i}{\rho_i}\right)}$$

Where the component's weight fraction (w_i) and density ρ_i are, respectively, and is the volume fraction of CuO in Equation (2.1). The “K” value in this model is more than 1.21 indicating poor adherence, whereas smaller values indicate enhanced adhesion. However, the aspect ratio and factor have been employed in the case of nanofiller to calculate the changed volume fraction according to Equation (2.2), and the modified volume fraction is now regarded as

$$\phi' = \phi_i \times \lambda \quad (2.1)$$

$$\lambda = a(A_f)^b \quad (2.2)$$

The aspect ratio (A_f) is assumed to be 5.71 in Equation (2.2). For various irregularities in nanocomposites, the amounts of “a” and “b” are improvement factors.

Model 2: A suggested power connection by Piggott-Leidner¹⁹ is given in the Equation (2.4), in which B indicates differences in stress concentration.

$$\text{RTS} = (1 - B\phi') \quad (2.4)$$

B stands for variations in stress concentration.

Model 3: According to Nielsen's model²⁰, which incorporates a stress concentration in expression, this model was built using the porosity theory (2.5).

$$\text{RTS} = e^{(-\tau\phi')} \quad (2.5)$$

The larger value in Equation (2.5) indicates poor adhesion due to a greater impact of stress concentration.

Model 4: A factor B related to interfacial qualities was included in the Turcsanyi model²⁰, as shown in Equation (2.6).

$$\text{RTS} = \frac{(1 - \phi')}{1 + 2.5 \times \phi'} \times e^{(B'\phi')} \quad (2.6)$$

The relative Young's modulus (RYM) is measured using a different set of theoretical models, and it is detailed below how the anticipated values from the trial and error procedure matched the experimental results.

Model 5: For adequate adhesion between a nanofiller and a polymer matrix, the modified Kerner model²¹ is applied as shown in Equation (2.7).

$$\text{RYM} = 1 + \frac{15(1 - \nu)\phi'}{(8 - 10\nu)(1 - \phi')} \quad (2.7)$$

The variable ν , which has a value of 0.4 in this equation, stands in for the polymer matrix's Poisson ratio. In addition, a correction factor and the impact of the aspect ratio of the CuO particles are taken into consideration in the updated volume fraction of filler.

Model 6: Halpin-Tsai model²² is typically for excellent adhesion and is provided by Equation (2.8).

$$\text{RYM} = \left[\frac{3(1 + 2\phi'\eta_e)}{8(1 - \phi'\eta_e)} + \frac{5(1 + 2\phi'\eta_T)}{8(1 - \phi'\eta_T)} \right] \quad (2.8)$$

$$\eta_e = \left[\frac{(\delta-1)}{(\delta+2A_f)} \right] \text{ and } \eta_T = \left[\frac{(\delta-1)}{(\delta+2)} \right]$$

In the equation above, the CuO modulus to PVA matrix modulus without CuO loading is the nanofiller, or ratio (δ).

Model 7: The Sato-Furukawa model²⁴ has the following model equation (2.9) and a symbol for an adhesion characteristic with a value between 0 (great adherence) and 1 (poor adherence)¹⁸.

$$\text{RYM} = \left[1 + \frac{(\phi')^{(2/3)}}{2(1 - (\phi')^{(1/3)})} (1 - \psi\xi) - \frac{(\phi')^{(2/3)}\psi\xi}{(1 - (\phi')^{(1/3)})\phi'} \right] \quad (2.9)$$

Where

$$\psi = \left(\frac{\phi'}{3} \right) \left[\frac{1 + (\phi')^{(1/3)} - (\phi')^{(2/3)}}{1 - (\phi')^{(1/3)} + (\phi')^{(2/3)}} \right]$$

3.0 Experimental Procedure

3.1 Preparation of Nano CuO particles

The solution combustion method is used to synthesize the nano-CuO particles. Glycine serves as the fuel, while copper (II) nitrate trihydrate serves as the precursor. The reaction mixture is typically prepared using distilled water as a solvent. The detailed synthesis procedure was described in the earlier paper¹⁹. The same work also discusses the characterization methods for the synthesized nano CuO particles, including FTIR, SEM, and XRD.

3.2 Nano CuO-PVA composite Films

Fabricating composite films using nanometal oxide (CuO) and polymer is accomplished by solution intercalation moulding (PVA). Initial preparation involves heating and stirring an aqueous solution with dissolving PVA granules for four hours at 80°C ($\pm 3^\circ\text{C}$). This solution has been mixed with synthetic nano-CuO powder. To homogenize the resulting suspension, it is ultrasonically processed for around 45 minutes at 85°C (minimum aggregation and homogeneous dispersion of nanoparticles in solution).



Figure 1: Fabrication mold used for nano CuO-PVA composite films

The resulting mixture was then quickly put into a glass mould that had been cleaned and dried, as shown in Figure 1. The mould is then dried for around 48 hours at 303°C in an environment free of dust. It was discovered that the dried films included uniformly distributed CuO nanoparticles free of any air bubbles. Solutions with variable concentrations of CuO nanoparticles (between 0 and 2% CuO by weight) were used to develop various films. The thickness of the prepared films, as determined by an LCD digital Vernier caliper, is reported to be between 0.19 and 0.21 mm. All films are made using 7.5% PVA suspensions.

3.3 Preparation of nano CdS particles

The hydrothermal process is used to produce the nano-CdS particles. Cadmium nitrate (precursor-1) is used as a precursor, Thiourea as fuel, L-valine (precursor-2) as a stabilizer, and to create the reaction mixture, deionized water is frequently employed as solvent. A detailed synthesis procedure was described in the earlier paper²⁰. Additionally, the same publication examined the characterization methods for the generated nano CuO particles, including FTIR, SEM, and XRD.

3.4 Nano CdS-PVA composite Films

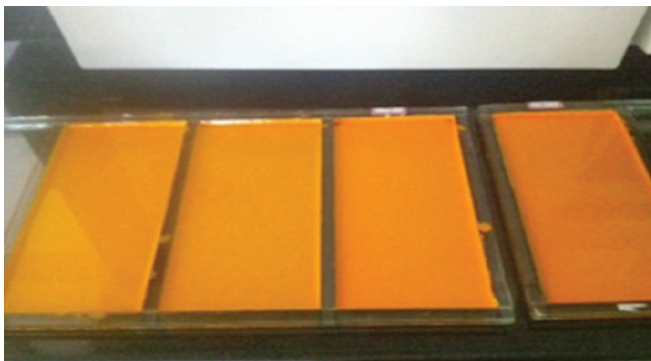


Figure 2: Fabrication mold used for nano CuO-PVA composite films

The process utilized to create the nano CdS-PVA composite is the same as that detailed in part 3.2. In the needed amount, nano CdS was added to the mixture in place of nano CuO material. Figure 2 displays the cast films that were maintained for dust-free air drying. The LCD digital Vernier caliper measured the height of dried manufactured films and found that it ranged from 0.18 to 0.22 mm.

4.0 Results and Discussion

4.1 Mechanical Properties

The mechanical properties of nanocomposite films were measured using the ASTM-recommended (KIPL-PC 2000; Error range: 0.2 MPa; Test rate for the gripping surface: 10 mm/min; Load cell: 0.2 kN) Universal Testing Machine. The specimen films employed ranged in thickness and breadth from 0.18 to 0.22 mm and 17 to 22 mm, respectively. Rectangular pieces measuring 3×1.95×0.02 cm³ were cut for tensile testing. The specimens of PVA and polymer composite films were broken by tensile testing.

By applying load to both synthesized polymer nanocomposite films and pure PVA films, stress-strain graphs were determined^{19,20}. The mechanical characteristics of PNCs samples, including ultimate tensile strength, flexural strength, Young's modulus, and toughness, were assessed using UTM tests. The tensile stress to tensile strain ratio, or Young modulus (E), is given as:

$$E = \frac{\text{tensile stress}}{\text{tensile strain}} = \frac{\sigma}{\epsilon} \quad (4.1)$$

4.2 Relative Tensile Strength of Nano CuO-PVA Composites Films

Figure 3, displays the relative tensile characteristics of the nano CuO-PVA composite as a function of the weight per cent of CuO input and comparison to theoretical and experimental values. According to Figure 3, the ultimate tensile strength of the nanocomposites increases linearly with the addition of

Table 2: Mathematical models for the RTS of nano CuO-PVA composites, including their values for the parameters a and b as well as their symbols

Model	a	b	Parameter value	Symbol
Piggot-Leidner	-2	1	10	B
Nicolais-Narkis	1.4	1	-4.1	K
Turcsanyi	-1.2	2	3	B'
Nielsen	-2.5	1	7	τ

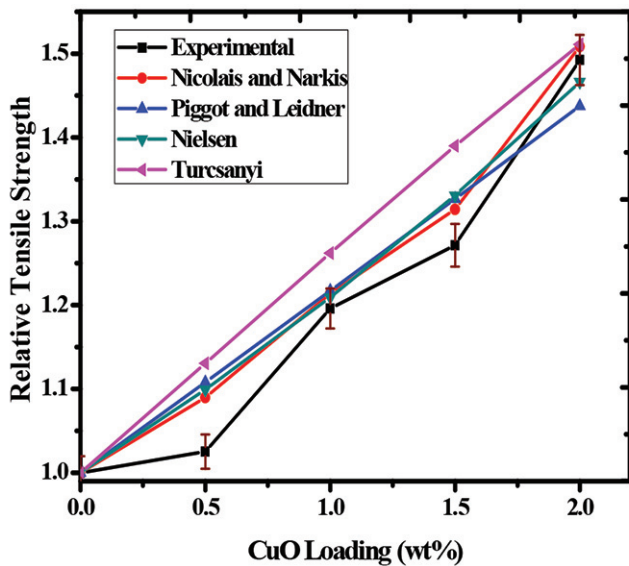


Figure 3: Deviation of relative tensile strength with CuO filler content in PVA

CuO. This improvement shows greater interfacial interactions between the nonpolar PVA and polar functionalized CuO, and it is caused by a blending of polymers that could boost their durability. However, as demonstrated, the blended nanocomposites have a higher relative tensile strength. This is due to the addition of CuO synthesized PVA that enhances linking blend components. Theoretical approaches are employed to analyze the dynamic and interactive characteristics and tensile strength.

Figure 3 displays the theoretical results of empirical studies along with the experimentally determined relative tensile strength. The Nicolais-Narkis model's predicted parameter value, which is $K=4.1$, shows a substantially lower than 1.21. Lower values imply strong adherence to the filler and polymer medium. According to^{21,22}, the Turcsanyi model's theoretical parameter value ($B'=3$) is more significant than 0.25, and this increased value implies strong adherence to the filler and polymeric matrix.

To forecast the mechanical characteristics of the nanocomposite, the experimental findings are contrasted with mathematical frameworks. Table 2 lists the predicted values for a, b, constants, and symbols for several models. These characteristic values suggest increased adhesion, which demonstrates good interfacial contacts between the interfaces of PVA and nanofiller and increases tensile strength. Indicating parameter values larger than 1.21 were the parameters B and from Piggot-Leidner ($B=10$) and Nielsen ($\tau=7$) models, correspondingly. The number 1.21 is relatively low, and rising levels signify worse adhesion. In contrast to the Piggot-Leidner model, the experimental results compared to empirical studies like the Nicolais-Narkis and Turcsanyi models reveal a close relationship with realistic values.

4.3 Relative Young's Modulus of Nano CuO-PVA Composites Films

Figure 4 depicts the relationship between CuO concentration and the relative tensile modulus of moulded nanocomposites (relative to Young's modulus). Theoretical findings show that RYM values somewhat increase with increasing CuO loading. Better interfacial interactions between the nanofiller and polymer are to blame for this. However, as seen in the image, adding nano-filler to a matrix significantly increased Young's modulus. Three current theories covered in this section employed values based on experimental data¹⁷.

The three possible parameters are represented in Table 4 by the values of a, b, and the typical parameter. The computed and displayed theoretical findings of RYM for different CuO loadings are presented in Figure 4. These models' anticipated theoretical values and experimentally obtained values agree rather closely. Additionally, the value of 0.6 denotes that the PVA matrix and nanofiller were iterated moderately²¹.

Table 3: Mathematical models for the RYM of nano CuO-PVA composites, including their values for the parameters a and b as well as their symbols

Model	a	b	Parameter value	Symbol
Sato-Furukawa	1.3	1.5	0.6	ξ
Halpin-Tsai	102	1	-	-
Kerner	1.2	1.5	-	-

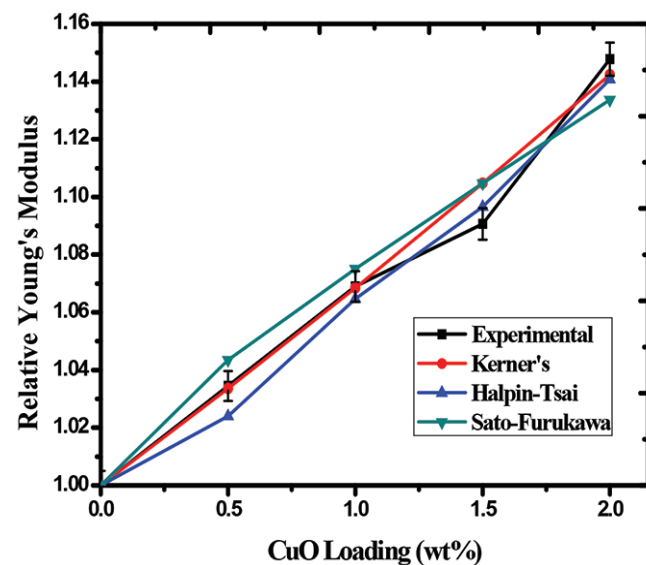


Figure 4: Variation in PVA's relative Young's modulus as a function of CuO filler content

It is said that low “ ξ ” creates a significant tensile modulus, demonstrating that an experimental calculation of a greater modulus is used. Increasing the interfacial bond between the substrate and nanoparticles, which transfers stress from the polymers to the nanofiller, the strongest and most elastic nanocomposites may be created.

4.4 Relative Tensile Strength of Nano CdS-PVA Composites Films

Figure 5 displays the relative tensile strength of nano CdS-PVA reinforced composites against the weight percentage of nano CdS loading (in contrast to actual and expected values). Nano CdS increases the UTS values, as seen in Figure 5. Theoretical constants obtained from models, such as Poisson’s ratio and aspect ratio ($A f$), are taken to be 10 and 0.4, respectively²³. The anticipated values for a, b, parameters, and symbols for various models are listed in Table 4.

Figure 4.3. displays the theoretical results from model parameters along with the experimentally determined relative tensile strength. The Nicolais-Narkis mathematical model value

Table 4: Mathematical models for the RTS of nano CdS-PVA composites, including their values for the parameters a and b as well as their symbols.

Model	a	b	Parameter value	Symbol
Piggot-Leidner	-1.2	1	12	B
Nicolais-Narkis	0.94	1	-5.5	K
Turcsanyi	-2.58	1.1	1	B'
Nielsen	-1.46	1	8	τ

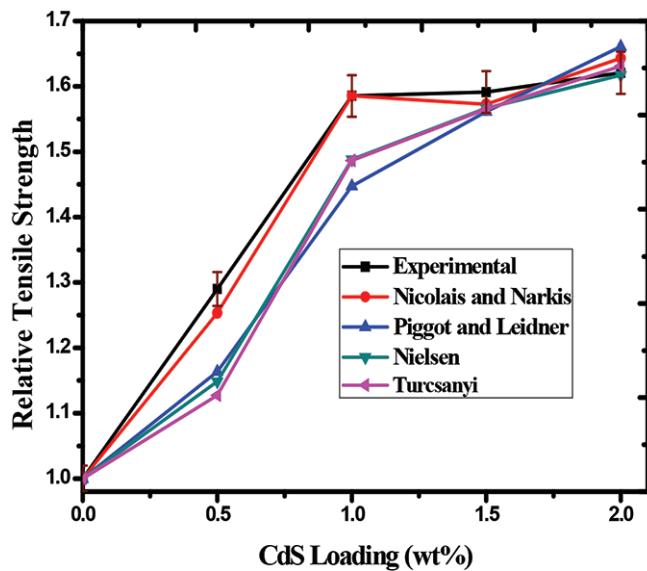


Figure 5: Variation in PVA's relative tensile strength as a function of CdS filler content

was calculated theoretically ($K = -5.5$), which is much smaller than (1.21). K values that are reduced imply good nanofiller and matrix adherence. The Turcsanyi model’s theoretical parameter value ($B' = 1$) indicates a parameter value greater than 0.25^{21,22}. Improved values imply strong adherence to the nanofiller and polymer substrate. The tensile strength values have increased due to the enhanced interfacial contacts between the surfaces of PVA and nanofiller shown by these model parameters, suggesting more excellent adhesion.

In the Nielsen ($\tau=8$) and Piggot-Leidner ($B=12$) models, respectively, the constants (B, τ) exhibited values larger than 1.21. The score of 1.21 is quite bad, and higher values signify worse adherence. The experimental results closely match actual values compared to empirical equations like the Nicolais-Narkis and Turcsanyi models. The Piggot-Leidner and Nielsen models do not accurately reflect experimental data.

4.5 Relative Young's Modulus of Nano CdS-PVA Composites Films

According to actual and theoretical data, Figure 4 compares composites containing CdS to cast NCs in terms of relative tensile properties (relative to Young's modulus). Theoretical results demonstrate a slight improvement in RYM values with increasing CdS loading. Enhanced interfacial bonding between the nanofiller and matrix is to blame for this. However, as seen in the image, adding nano-filler to a matrix considerably increases Young’s modulus.

The three models and their constants are represented by the values of a, b, and the typical parameter values listed in Table 5. Figure 6 illustrates the theoretically computed values obtained from mathematical frameworks. These models' projected theoretical values are relatively close to their experimental ones. Furthermore, the value of is 0.2 indicates an excellent interaction between the added nanofiller and the PVA matrix.

It is stated that “ ξ ” creates a significant tensile modulus, showing that a greater modulus was determined through experimental testing. Enhancing the interfacial bonding between the matrix and nanoparticles, which transmits stress from the matrix to the fillers, results in composites with the

Table 5: Mathematical models for the RYM of nano CdS-PVA composites, including their values for the parameters a and b as well as their symbols

Model	a	b	Parameter value	Symbol
Sato-Furukawa	15.66	1	0.2	
Halpin-Tsai	2	3.3	-	-
Kerner	10.64	1	-	-

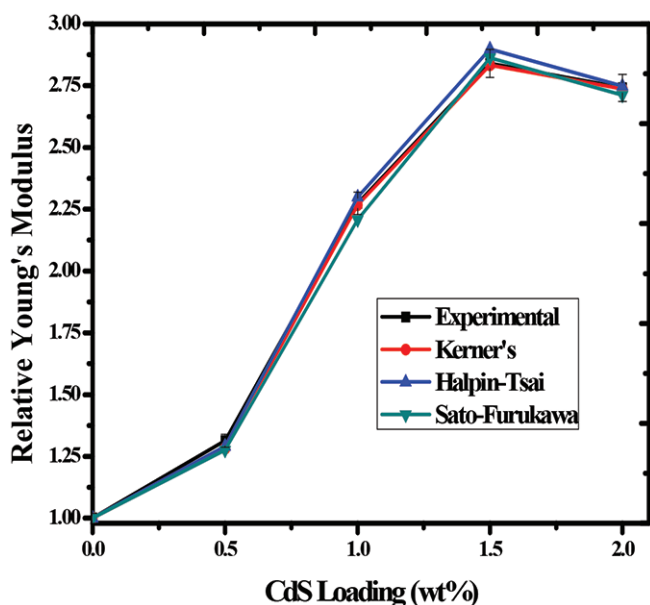


Figure 6: Deviation of relative Young's modulus with CdS filler content in PVA

highest strength and modulus. All of the possible models have strong relationships with the results obtained.

5.0 Conclusions

CuO and CdS Nanoparticles were synthesized by solution combustion method. Characterization techniques used XRD for crystallinity and SEM for surface morphology. Different PNC films were cast with different wt% of nanoparticles in the range of 0-2 wt%. Mechanical properties were obtained using UTM, Further the comparison between experimental values and theoretical values using mathematical models.

In particular, the Turcsanyi, Nielsen, Piggot-Leidner, and Nicolais-Narkin models for relative tensile strength, as well as Young's modulus, were utilized in calculations on films made of nanocubes of CuO and PVA. The model parameter K obtained as -4.1, which is less than 1.21, indicated good adhesion. Other parameters $B=10$ and $\tau=7$ were more significant than 1.21, showing poor adhesion. In comparison with the Piggot-Leidner model, the Nicolais-Narkis and Turcsanyi models showed experimental findings that more closely matched their predictions. Kerner, Halpin-Tsai, and Sato-Furukawa model-based estimations of the relative Young's modulus have good agreement with experimental results. The value ξ obtained was 0.6 suggesting moderate interaction with nanofiller and PVA matrix. The low " ξ " makes a great tensile modulus, Kerner model, and experimental results show a fair degree of agreement.

Similarly, the relative tensile strength and Young's modulus on fabricated Nano CdS-PVA composite films were

estimated using the same models. The obtained parameter values of K (-5.5) are less than 1.21, indicating good adhesion. Other parameter values B (12) and τ (8) are more significant than 1.21, showing poor adhesion. The Nicolais-Narkis and Turcsanyi models predicted better than Piggot-Leidner model. The values obtained from the Turcsanyi and Nicolais-Narkin designs also agreed well with the calculated observations. The forecasting of the Piggot-Leidner and Nielsen models did not agree well. The very excellent relationship between the added CdS nanoparticle and the PVA substrate is suggested by the relative Young's modulus calculated using the Kerner, Halpin-Tsai, and Sato-Furukawa models, and the value of 0.2 achieved is also in good conformity with experimental results.

6.0 References

1. Li, X., Wang, X., Zhang, L., Lee, S., and Dai, H. (2008); Chemically derived, ultrasmooth graphene nanoribbon semiconductors science, 319, 5867, 1229-1232.
2. Ash, Benjamin J., Richard W. Siegel, and Linda S. Schadler. (2004): Glass-transition temperature behaviour of alumina/PMMA nanocomposites. *Journal of Polymer Science Part B: Polymer Physics*, 42, 23, 4371-4383.
3. P, Rathnakar.G and Pal Pandian. (2015): A Review on the Use and Application of Polymer Composites in Automotive Industries. *International Journal for Research in Applied Science & Engineering Technology (IJRASET)*, 3, 4, 898-902.
4. Weickmann, H., Tiller, J. C., Thomann, R., & Mülhaupt, R. (2005): Metallized organoclays as new intermediates for aqueous nanohybrid dispersions, nanohybrid catalysts and antimicrobial polymer hybrid nanocomposites. *Macromolecular Materials and Engineering*, 290, 9, 875-883.
5. Chen, S. and Sommers, J. M. (2001): Alkanethiolate-protected copper nanoparticles: spectroscopy, electrochemistry, and solid-state morphological evolution. *The Journal of Physical Chemistry B*, 105, 37, 8816-8820.
6. Sousa, M. H., Tourinho, F. A., Depeyrot, J., da Silva, G. J. and Lara, M. C. F. (2001): New electric double-layered magnetic fluids based on copper, nickel, and zinc ferrite nanostructures. *The Journal of Physical Chemistry B*, 105, 6, 1168-1175.
7. Niederberger, M., Garnweitner, G., Buha, J., Polleux, J., Ba, J. and Pinna, N. (2006): Nonaqueous synthesis of metal oxide nanoparticles: Review and indium oxide as case study for the dependence of particle morphology on precursors and solvents. *Journal of Sol-Gel Science and Technology*, 40, 2-3, 259-266.

8. Wu-Song Huang, Brian D. Humphrey and Alan G. (1986): MacDiarmid. Polyaniline, a novel conducting polymer. Morphology and chemistry of its oxidation and reduction in aqueous electrolytes. *Journal of the Chemical Society, Faraday Transactions 1: Physical Chemistry in Condensed Phases*, 82, 8, 2385-2400.
9. Demczyk, B. G., Wang, Y. M., Cumings, J., Hetman, M., Han, W., Zettl, A. and Ritchie, R. O. (2002): Direct mechanical measurement of the tensile strength and elastic modulus of multiwalled carbon nanotubes. *Materials Science and Engg: A*, 334, 1-2, 173-178.
10. Deepthi, M. V., Sharma, M., Sailaja, R. R. N., Anantha, P., Sampathkumaran, P., & Seetharamu, S. (2010): Mechanical and thermal characteristics of high density polyethylene-fly ash cenospheres composites. *Materials & Design*, 31, 4, 2051-2060.
11. Willett, J. L. (1994): Mechanical properties of LDPE/granular starch composites. *Journal of Applied Polymer Science*, 54, 11, 1685-1695.
12. Bliznakov, E.D., White, C.C., and Shaw, M.T. (2000): Mechanical properties of blends of HDPE and recycled urea?formaldehyde resin. *Journal of Applied Polymer Science*, 77, 14, 3220-3227.
13. Raju, G.M., Madhu, G.M., Khan, M.A. and Reddy, P. D.S. (2018): Characterizing and Modeling of Mechanical Properties of Epoxy Polymer Composites Reinforced with Fly ash. *Materials Today: Proceedings*, 5(14), 27998-28007., 5, 14, 27998-28007.
14. Raju, G. M., Dakshayini, B. S., Madhu, G. M., Khan, M. A., & Reddy, P.D.S. (2018): Characterizing and Modeling of Mechanical Properties of Epoxy Polymer Composites Reinforced with Bentonite Clay. *Materials Today: Proceedings*, 5, 14, 28098-28107.
15. Falqi, F. H., Bin-Dahman, O. A., Hussain, M., & Al-Harhi, M. A. (2018): Preparation of Miscible PVA/PEG Blends and Effect of Graphene Concentration on Thermal, Crystallization, Morphological, and Mechanical Properties of PVA/PEG (10 wt%) Blend. *International Journal of Polymer Science* 2018.
16. Liang, J., Huang, Y., Zhang, L., Wang, Y., Ma, Y., Guo, T., and Chen, Y. (2009): Molecular-level dispersion of graphene into poly (vinyl alcohol) and effective reinforcement of their nanocomposites. *Advanced Functional Materials*, 19, 14, 2297-2302.
17. Rao JK, Raizada A, Ganguly D, Mankad M, Satyanarayana SV, Madhu GM. (2015): Enhanced mechanical properties of polyvinyl alcohol composite films containing copper oxide nanoparticles as filler. *Polymer Bulletin*, 7071-65.
18. Nicolais, L., and Narkis, M. (1971): Stress-strain behaviour of styrene?acrylonitrile/glass bead composites in the glassy region. *Polymer Engineering & Science*, 11, 3, 194-199.
19. Piggott, M. R. and Leidner, J. (1974): Misconceptions about filled polymers. *Journal of applied polymer science*, 18, 6, 1619-1623.
20. Nielsen, L. E. (1966): Simple theory of stress-strain properties of filled polymers. *Journal of Applied Polymer Science*, 10, 1, 97-103.
21. Turcsanyi, B., Pukanszky, B. and Tüdös, F. (1988): Composition dependence of tensile yield stress in filled polymers. *Journal of Materials Science Letters*, 7, 2, 160-162.
22. Kerner, E. H. (1956): The elastic and thermo-elastic properties of composite media. *Proceedings of the physical society. Section B*, 69, 8, 808.
23. J.C. Halpin and S.W. Tsai. (1967): "Effect of Environmental Factors on Composite Materials" Air Force Technical Report. Dayton, OH, 1967.
24. Sato, Y. and Furukawa, J. (1963): A molecular theory of filler reinforcement based upon the conception of internal deformation (a rough approximation of the internal deformation). *Rubber chemistry and technology*, 36, 4, 1081-1106.
25. Zare, Yasser. (2014): Determination of polymer-nanoparticles interfacial adhesion and its role in shape memory behaviour of shape memory polymer nanocomposites. *International Journal of Adhesion and Adhesives*, 54, 67-71.
26. J. K. Rao, A. Raizada, D. Ganguly, M. Mankad, S. V. Satyanarayana and G. M. Madhu. (2015): Investigation of structural and electrical properties of novel CuO-PVA nanocomposite films,. *Journal of Material Science*, 50, 21, 7064 -7074.
27. J. Koteswararao, R. Abhishek, S. V. Satyanarayana, G. M. Madhu and V. Venkatesham. (2016): Influence of cadmium sulfide nanoparticles on structural and electrical properties of polyvinyl alcohol films,. *EXPRESS Polymer Letters*, 10, 11, 883-894.
28. V.C. Divya, M. Ameen Khan, B. Nageshwar Rao, R.R.N. Sailaja. (2015): High density polyethylene/cenosphere composites reinforced with multi-walled carbon nanotubes: Mechanical, thermal and fire retardancy studies. *Materials and Design*, 65, 377-386.
29. Evelin D. Bliznakov, Chris C. White, Montgomery T. Shaw. (2000): Mechanical Properties of Blends of HDPE and Recycled Urea-Formaldehyde Resin. *Journal of Applied Polymer Science*, 77, 3220-3227.
30. Jorg Rockenberger, Larc Trogera, Andrey L. Rogachb, Markus Tischer, Marius Grundmann, Alexander Eychmuller and Horst Wellera. (1998): The contribution of particle core and surface to strain, disorder and vibrations in thiolcapped CdTe nanocrystals. *Journal of Chemical Physics*, 108, 18, 7807-7815.
31. Yasser Zare, Hamid Garmabi. (2015): A developed model to assume the interphase properties in a ternary polymer nanocomposite reinforced with two nanofillers. *Composites Part B*, 75, 29-35.